

Thermoelectric Properties of the SmCoO₃ and NdCoO₃ Cobalt Oxides

V. A. Dudnikov¹, A. S. Fedorov^{1,4}, Yu. S. Orlov^{1,4}, L. A. Solovyov², S. N. Vereshchagin²,
S. Yu. Gavrilkin³, A. Yu. Tsvetkov³, M. V. Gorev^{1,4}, S. V. Novikov⁵, and S. G. Ovchinnikov^{1,4}

¹Kirensky Institute of Physics, Krasnoyarsk Scientific Center, Siberian Branch, Russian Academy of Sciences, Krasnoyarsk, 660036 Russia

²Institute of Chemistry and Chemical Technology, Krasnoyarsk Scientific Center, Siberian Branch, Russian Academy of Sciences, Krasnoyarsk, 660036 Russia

³Lebedev Physical Institute, Russian Academy of Sciences, Moscow, 119991 Russia

⁴Siberian Federal University, Krasnoyarsk, 660041 Russia

⁵Ioffe Institute, St. Petersburg, 194021

The thermoelectric properties of the NdCoO₃ and SmCoO₃ rare-earth cobalt oxides with a perovskite structure have been investigated in a wide temperature range. It is shown that, in the low-temperature region, the thermal conductivity of the compounds has a sharp maximum and the electrical conductivity of the samples increases with temperature, whereas the Seebeck coefficient behaves nonmonotonically with increasing temperature. The SmCoO₃ oxide is characterized by the positive thermopower over the entire investigated range with a sharp growth in the low-temperature region, attaining the maximum value ($S \approx 1000 \mu\text{V/K}$) near room temperature, and a further decrease. It has been established that, in the NdCoO₃ oxide, the Seebeck coefficient changes its sign, which was rarely observed in the La-based compounds and is atypical of the undoped rare-earth cobalt oxides. The thermopower maximum obtained at a temperature of 450 K is $400 \mu\text{V/K}$. The regions of the fastest growth of the thermoelectric power factor correspond to the anomalies caused by the spin transition of Co³⁺ ions and the dielectric–metal transition.

1. Introduction

Despite the long-term investigations of the LnCoO₃ (Ln = La, rare-earth metal) cobalt oxides [1, 2], there still has been a keen interest in these compounds due to their unique physical properties and high application potential. The features of their magnetic, transport, thermodynamic, and other properties originate from the competition of different spin states of the Co³⁺ ion, which is caused by the similarity of the intraatomic exchange coupling and crystal field energy, and depend on the external factors, including temperature and pressure. In these materials, cobalt ions can be in the low-spin (LS, $S = 0$, t_{2g}^6), intermediate-spin (IS, $S = 1$, $t_{2g}^5 e_g^1$), and high-spin (HS, $S = 2$, $t_{2g}^4 e_g^2$) states. The role of an external pressure can be played by the chemical pressure induced upon substitution of one lanthanide for another in the LnCoO₃ composition, which leads to either stabilization or destabilization of the ground low-spin state of Co³⁺ ions, depending on the ionic radius of a substitute [3,4,5]. New data on the features of the physicochemical properties of these compounds are regularly reported. Ikeda et al. [6] studied the LaCoO₃ oxide in ultra-strong (up to 133 T) magnetic fields at different temperatures and established an extraordinary field dependence of magnetization. In [7, 8], it was shown that the oxygen nonstoichiometry of the samples increases with a decrease in the ionic radius of the rare-earth

element and the perovskites become less stable, which is consistent with a decrease in the tolerance factor t

$$t = \frac{r_{Ln} + r_O}{\sqrt{2}(r_{Co} + r_O)} \quad (r_{Ln}, r_O, \text{ and } r_{Co} \text{ are the lanthanide, oxygen, and cobalt ionic radii, respectively})$$

characterizing the LnCoO_3 perovskite material and reflecting the distortion of the oxygen octahedron CoO_6 and change in the Co–O bond lengths and Co–O–Co angles.

In addition, the recent studies have been devoted to the development of new sample fabrication techniques [9, 10], behavior of the properties of samples under the hydrostatic and chemical pressure [11], and possibility of application [12]. The LnCoO_3 oxides with a perovskite structure are good candidates for use in gas-sensing media, since they rapidly response to the change in the gas composition and have the high chemical and structural stability under long-term exposure to alternating gases [13]. The undoped LnCoO_3 cobalt oxides have a fairly high Seebeck coefficient near room temperature [14,15,16] and the absence of toxic elements in their composition, stability against oxidizing media at high temperatures, and possibility of various substitutions in these compounds for modifying their properties make them promising for use as thermoelectric materials capable of converting geothermal or waste heat to the electric energy. The thermoelectric properties of the rare-earth cobalt oxides are usually investigated in the region above room temperature. Studies of the thermoelectric properties of these compounds at lower temperatures have been rarely met [17,18,19,20,21] and the cases of observation of the n -type conductivity of the LnCoO_3 compounds are few and concern mainly the LaCoO_3 oxide [18-22].

The aim of this work was to examine the thermoelectric properties of still understudied SmCoO_3 and NdCoO_3 cobalt oxides in a wide temperature range. One may expect that the strong fluctuations of the multiplicity, i. e., switching between the high- and low-spin states of cobalt, will be favorable for improving the thermoelectric properties of the compounds, since the switching of the spin state leads to the rearrangement of the electronic structure and change in the conductivity type. On the other hand, the great (about 10%) difference between the ionic radii of the high- and low-spin Co^{3+} ions causes the anomalies in the temperature dependence of the lattice parameters and heat expansion, which necessarily affects the thermal conductivity.

2. Experimental

The NdCoO_3 and SmCoO_3 samples were prepared by the conventional solid-state synthesis from the high-purity Co_3O_4 , Nd_2O_3 , and Sm_2O_3 oxides taken in stoichiometric amounts at 1100°C for 36 h. The procedure involved triple intermediate grinding, final grinding of the mixture, and pressing in tablets 20 mm in diameter with a thickness of 2 mm. The tablets were annealed at 1200°C for 8 h and cooled in a furnace to room temperature at a rate of $2^\circ\text{C}/\text{min}$. The measurements were performed on bars $5 \times 13 \times (1-2) \text{ mm}^3$ in size cut from the tablets.

The X-ray diffraction analysis (XRD) was made on a PANalytical X'PertPRO powder diffractometer (Netherlands) in $\text{CoK}\alpha$ radiation; the shooting was performed at room temperature in the 2θ angle range of $0-130^\circ$. The LnCoO_3 ($\text{Ln} = \text{Nd}, \text{Sm}$) samples were grinded in an agate mortar in octane, dried, and placed in a flat holder for the XRD measurements in the Bragg-Brentano geometry. The crystal structure was refined using the full-profile XRD pattern by the derivative difference minimization (DDM) method [23].

The low-temperature investigations were carried out on a Quantum Design Physical Property Measurement System (PPMS-9) at the Center for Collective Use, Lebedev Physical Institute, Russian Academy of Sciences (Moscow). The high-temperature measurements were performed on a thermopower and resistance measurement setup [24] at the Ioffe Institute (St. Petersburg).

The thermal expansion of the samples was studied on a Netzsch DIL-402C induction dilatometer at temperatures of 100–700 K in the dynamic mode at a heating and cooling rate of 3 K/min at the dry helium purging (the volume content of oxygen is $O_2 \approx 0.05\%$).

3. Results and discussion

According to the XRD data, the $SmCoO_3$ and $NdCoO_3$ samples had a perovskite-type single-phase rhombically distorted structure with sp. gr. $Pbnm$ (Fig. 1), which is typical of the $LnCoO_3$ compounds.

The room-temperature lattice parameters are consistent with the literature data from [25, 26], but somewhat differ from the data for $SmCoO_3$ reported in [27]. The maximum similarity with the data obtained in [11] is observed. The crystal lattice parameters at $T = 300$ K are given in Table 1. Fig. 2 shows micrographs of the studied sample surfaces. The grain size for $NdCoO_3$ is significantly larger than for $SmCoO_3$ (Fig 2). This, accordingly, affects the density and porosity (Table 2).

Figure 3 presents temperature dependences of the thermal conductivity for the $LaCoO_3$, $NdCoO_3$, and $SmCoO_3$ samples together with the data on $LaCoO_3$ borrowed from [22] for comparison. In the low-temperature ($T < 50$ K) region, the dependences of all the samples have a maximum, which shifts toward higher temperatures with an increase in the radius of the rare-earth Ln^{3+} ion. The ground state of cobalt ions is beyond question and determined as a nonmagnetic LS state and the series of electron spin resonance (ESR) experiments [28] and X-ray spectroscopy studies [29] of the $NdCoO_3$ and $SmCoO_3$ compositions revealed the transition of cobalt ions from the low- to high-spin state at temperatures much higher than the temperatures of the observed maxima. Therefore, it seems reasonable to attribute this maximum to the growth of the oxygen nonstoichiometry of the samples with a decrease in the lanthanide ionic radius [7,8] accompanied by the perovskite structure distortion and to the possible formation of dimers considered in [28] for the $SmCoO_3$ compound, rather than to the change in the spin state of cobalt ions, as was made in [22].

Our data on the absolute values of the total thermal conductivity of $NdCoO_3$ at $T = 350$ K are consistent with the results of the high-temperature investigations of the thermal conductivity from [14]. The analysis of the data reported in [22] and [14] allow us to conclude that, at intermediate temperatures of 450–700 K, a blurred minimum arises in some rare-earth cobalt oxides, which is followed by the thermal conductivity growth with increasing temperature.

Figure 4 shows temperature dependences of the Seebeck coefficient for the samples under study. It is worth noting that the low-temperature (up to 350 K) and high-temperature (above 350 K) measurements were performed on different facilities. The absence of discrepancies at the coupling temperatures is indicative of the high quality of the measurements and reliability of the data obtained.

The deviation from the zero thermopower for the $SmCoO_3$ compound is observed at a temperature of 200 K; after that, the thermopower is positive over the entire measurement range.

It means that the SmCoO_3 compound is a p -type semiconductor and the majority carriers are holes. At 230 K, the Seebeck coefficient starts sharply growing and attains its maximum (about $1000 \mu\text{V/K}$) near room temperature. Then, the Seebeck coefficient monotonically decreases with increasing temperature and has a kink around 450 K; above this temperature, it drops to its minimum values. The behavior of the Seebeck coefficient of NdCoO_3 in the low-temperature region is drastically different. The deviation from the zero value is observed a bit earlier than in the case of SmCoO_3 , but the thermopower passes to the negative region and has a minimum of $-210 \mu\text{V/K}$ at $T = 275 \text{ K}$, which points out the dominance of the n -type conductivity in this temperature range. As the temperature increases, the thermopower takes positive values above 350 K and has a maximum ($400 \mu\text{V/K}$) at $T = 450 \text{ K}$ with a further smooth decrease.

Change of sign on temperature dependences of the Seebeck coefficient for perovskite-like compounds it is usually observed in rare-earth cobaltites with heterovalent substitution or in the partial replacement of cobalt ions by tetravalent metal ions.

A similar phenomenon was observed in the $\text{Gd}_{1-x}\text{Sr}_x\text{CoO}_{3-\delta}$ compounds [29], the $\text{LaCo}_{1-x}\text{Ti}_x\text{O}_3$ samples in which Ti^{4+} doping induces additional electron carriers in the Co–O subsystem [18], and the $\text{RBaCo}_2\text{O}_{5+x}$ ($\text{R} = \text{Gd}, \text{Nd}$) compounds [30] in which the change in the sign in the temperature dependences of the Seebeck coefficient was attributed to the change in the oxygen nonstoichiometry.

The negative thermopower values in the undoped rare-earth cobalt oxides and at the isovalent substitution are rarely met and related mainly to the lanthanum-based compounds [18,20,21]. In [22] when studying LaCoO_3 single crystals grown under the same conditions, either a large negative or a large positive Seebeck coefficient was obtained at temperatures below 300 K. The authors attributed this to the high sensitivity of thermopower even to very small deviations of the oxygen content and weak inhomogeneities in the distribution of oxygen over the volume of the sample, which can strongly affect the sign and magnitude of thermopower. Most likely, the negative Seebeck coefficient for NdCoO_3 obtained in our experiment is connected with these reasons. However, the difference in the signs of thermopower can also be associated with contamination with impurity elements [19] or with a deviation from the stoichiometric composition of cations [39].

Figure 5 shows temperature dependences of the electrical conductivity for the synthesized samples. The behavior of the conductivity corresponds to the semiconductor type; i. e., the conductivity increases with temperature.

The comparison of the electrical conductivity at fixed temperatures shows that the σ value for the SmCoO_3 compound is systematically lower than the value for the NdCoO_3 compound and its absolute value at high temperatures lies between the values for Nd^{3+} and Tb^{3+} [14], which confirms a decrease in the electrical conductivity of the unsubstituted rare-earth cobalt oxides with a decrease in the ionic radii of the rare-earth elements. According to the experimental data and results from [14,16,17,27, 31], the conductivity values form a series $\sigma_{\text{La}} > \sigma_{\text{Pr}} > \sigma_{\text{Nd}} > \sigma_{\text{Sm}} > \sigma_{\text{Gd}} > \sigma_{\text{Tb}} > \sigma_{\text{Dy}}$. This dependence is explained by the unit cell distortion, which leads to a decrease in the Co–O bond lengths and Co–O–Co bond angles and, correspondingly, to a decrease in the overlap of the cobalt $3d$ orbitals and oxygen $2p$ orbitals [32, 33]. This results in the so-called lanthanide compression, which stabilizes the low-spin state of Co^{3+} ions, and the shift of the blurred semiconductor–metal transition and other features toward higher temperatures [3, 34].

The electrical conductivity of perovskite with zero porosity σ_{per} can be calculated from experimental data by the formula [7,38] $\sigma_{per} = \frac{2}{3(1-P - \frac{1}{dim})} \sigma_{exp}$, where σ_{per} is the perovskite electrical conductivity, P is the calculated porosity, dim is the dimension (for a bulk sample $dim = 3$), and σ_{exp} is the experimental electrical conductivity.

Corrected thermal conductivity for samples with 100% density without taking into account the real pore structure (pore size distribution and morphology) can be determined from the ratio [40, 41]

$k_{per} = \frac{k_{exp}}{(1-P)}$, where k_{per} is the corrected thermal conductivity at 100% density, k_{exp} is the measured thermal conductivity and P is the porosity.

It should be noted that the porosity of the studied samples is quite high. Therefore, the corrected thermal conductivity k_{per} significantly exceeds the obtained experimental values, and the electrical conductivity σ_{per} , on the contrary, is much smaller.

Figure 6 shows temperature dependences of the anomalous contributions to the thermal expansion coefficient and the thermoelectric power factors for (a) the NdCoO₃ and (b) SmCoO₃ compounds. The first anomaly in the volumetric thermal expansion coefficient is related to the transition of Co³⁺ ions from the low- to high-spin state and corresponds to the maximum rate of population of the high-spin state $dn_{HS}(T)/dT$, where $n_{HS}(T)$ is the temperature-dependent probability of population of the high-spin state of Co³⁺ ions, which is determined as $n_{HS}(T) = \frac{g_{HS} \exp(-\Delta_S / k_B T)}{1 + g_{HS} \exp(-\Delta_S / k_B T)}$, where k_B is the Boltzmann constant, T is the temperature, and g_{HS} is the degree of degeneracy of the term ⁵T_{2g} determined by spin S and orbital moment L (for the Co³⁺ ion, we have $S = 2$, $L = 1$, $g = (2S + 1)(2L + 1) = 15$) [37]. (This anomaly for SmCoO₃ is shown, for clarity, by crossing of the straights in Fig. 5 6 b). The high-temperature maximum is related to the smooth dielectric–metal transition, which occurs in all rare-earth cobalt oxides upon their heating [4,5,15,25].

The temperature dependences of the thermoelectric power factor $P = S^2\sigma$ determined by the electronic properties of the material (thermopower S and electrical conductivity σ) show the correlation with the anomalies observed upon thermal expansion of the samples. The plots include two portions of the rapid growth of the power factor. The first region corresponds to the low-temperature anomaly of the thermal expansion and is therefore related to the spin transition of Co³⁺ ions. The second region correlates with the high-temperature $\beta(T)$ anomaly and, consequently, the dielectric–metal transition. In this case, the regions of the maximum growth of the power factor also repeat a trend to shifting toward higher temperatures with decreasing ionic radius of the rare-earth element. This result can be used in fabrication of materials for the thermoelectric energy conversion in systems with strong electron correlations.

4. Conclusions

We investigated the thermoelectric properties of the NdCoO₃ and SmCoO₃ rare-earth cobalt oxides with a perovskite structure in a wide temperature range. It was found that the electrical conductivity of the samples increases with temperature, while the Seebeck coefficient behaves nonmonotonically as the temperature increases. The SmCoO₃ compound is characterized by the positive thermopower over the entire temperature range with a sharp

increase in the low-temperature region, formation of a maximum ($S \approx 1000 \mu\text{V/K}$) near room temperature, and a further drop. For the NdCoO_3 compound, we disclosed the unique change in the Seebeck coefficient sign, which is rarely observed in the La-based compounds and atypical of the undoped cobalt oxides. In this case, the thermopower maximum ($400 \mu\text{V/K}$) is attained at 450 K. The thermoelectric power factor P for the NdCoO_3 oxide is more than twice as much as for the SmCoO_3 oxide. The regions of the fastest growth of the power factor correspond to the anomalies caused by the spin transition of Co^{3+} ions (the first anomaly in the heat expansion) and the dielectric–metal transition (the high-temperature anomaly in the heat expansion) and repeat a trend to shifting toward higher temperatures with decreasing ionic radius of the rare-earth element. Our investigations essentially supplement the previous studies of the thermoelectric properties of the undoped rare-earth cobaltites and confirm the rare-earth cobalt oxides to be promising materials for the thermoelectric energy conversion.

Funding

This study was supported by the Russian Science Foundation, project no. 16-13-00060.

Figures and Tables

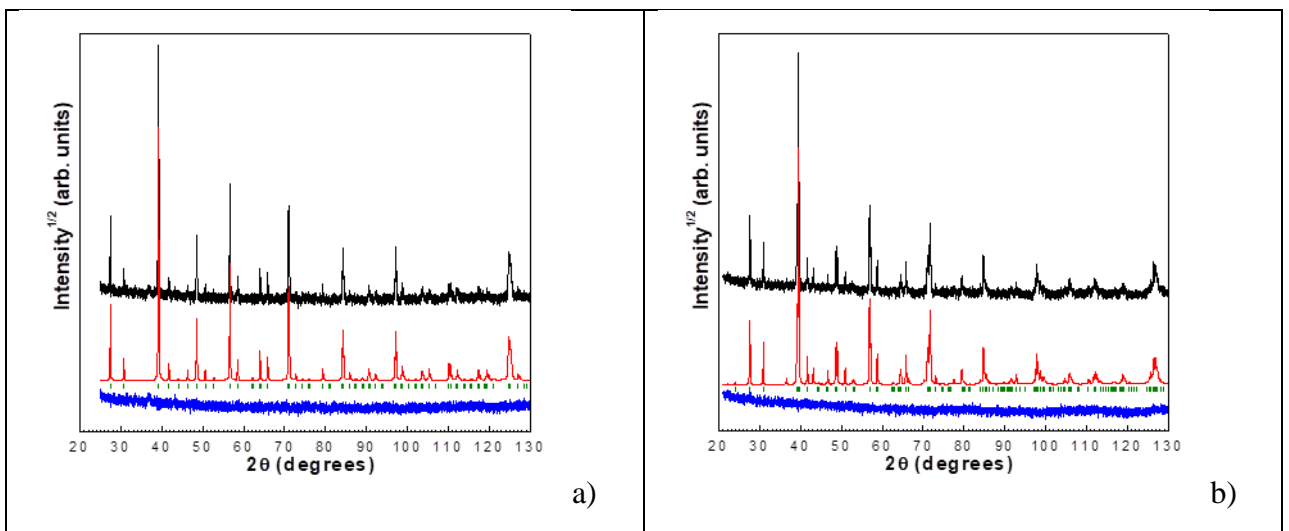


Fig. 1. Experimental (upper black), calculated (middle red), and difference (lower blue) XRD profiles for (a) the NdCoO_3 and (b) SmCoO_3 compounds at 300 K.

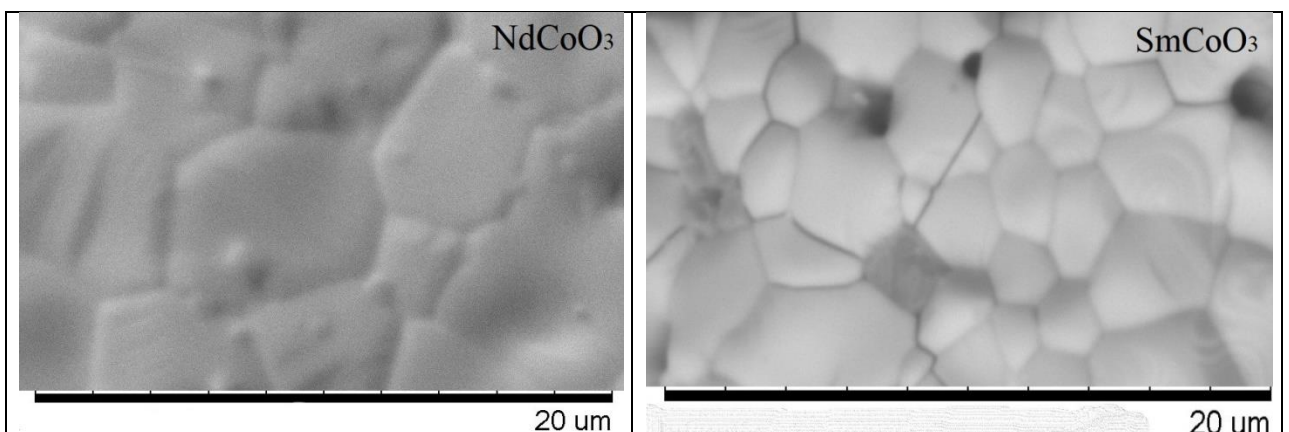


Fig.2. Micrographs of the surface of perovskites NdCoO_3 and SmCoO_3 .

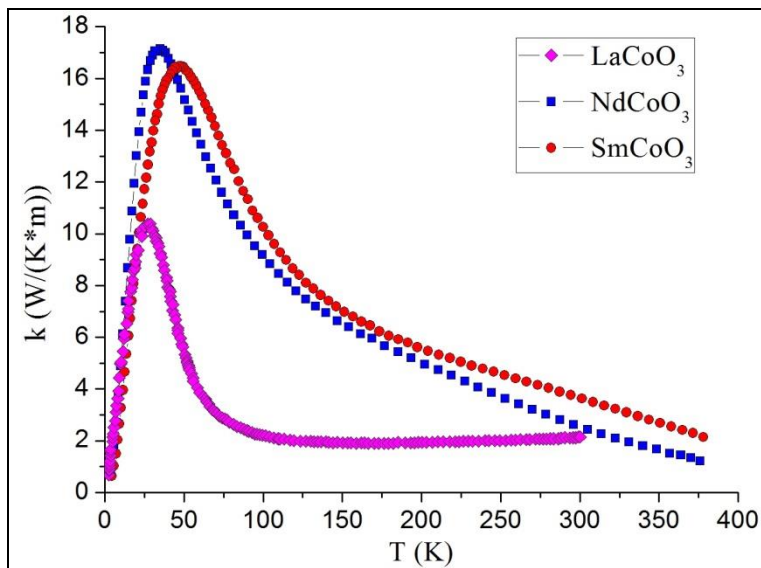


Fig. 3. Temperature dependences of specific heat for the LnCoO_3 ($\text{Ln} = \text{La}$, purple rhombs), Nd (blue squares), and Sm (red circles) samples. The data on LaCoO_3 were borrowed from [22] for comparison.

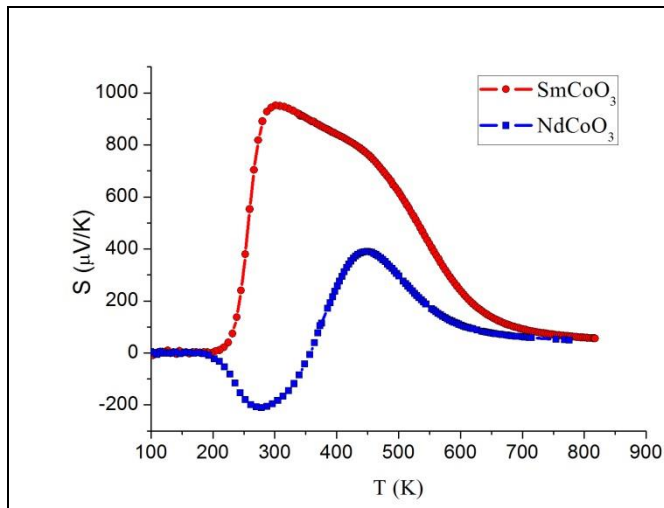


Fig. 4. Temperature dependences of the Seebeck coefficient for the NdCoO_3 (blue squares) and SmCoO_3 (red circles) samples.

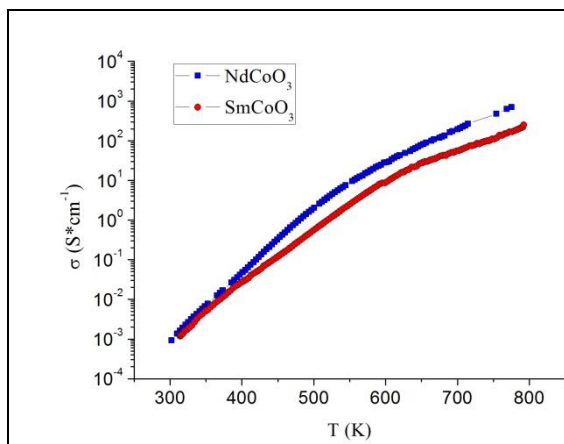


Fig. 5. Temperature dependences of the electrical conductivity for the NdCoO_3 (blue squares) and SmCoO_3 (red circles) samples.

a)

b)

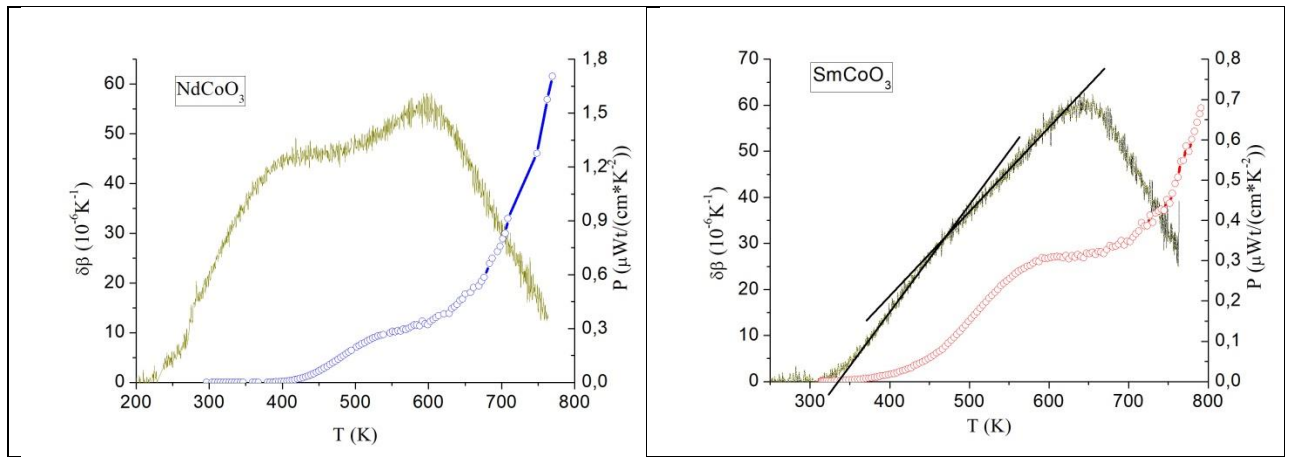


Fig. 6. Temperature dependences of the anomalous contributions to the thermal expansion coefficient and thermoelectric power factors for (a) the NdCoO₃ and (b) SmCoO₃ samples. For SmCoO₃, the crossing of the straights corresponds to the temperature of the maximum rate of the population of the high-spin state.

	a , Å	b , Å	c , Å	V , Å ³
NdCoO ₃	5.3478(1)	5.3324(1)	7.5505(2)	215.32(1)
SmCoO ₃	5.2887(1)	5.3517(3)	7.5031(2)	212.37(1)

Table 1. The NdCoO₃ and SmCoO₃ crystal lattice parameters at room temperature

	ρ_{per} (g/cm ³)	ρ_{exp} (g/cm ³)	Porosity P (%)	k_{per}/k_{exp}	$\sigma_{per}/\sigma_{exp}$
NdCoO ₃	7.75	5.60	27.66	1.38	0.84
SmCoO ₃	8.05	5.36	33.36	1.50	0.86

Table 2. Theoretical density of the NdCoO₃ and SmCoO₃ calculated from crystallographic data ρ_{per} , experimental density ρ_{exp} , porosity P and coefficients relating normalized and experimental values of thermal conductivity (k_{per}/k_{exp}) and electrical conductivity ($\sigma_{per}/\sigma_{exp}$) at $T = 300$ K.

References

- [1] B. Raveau, M. Seikh, Cobalt Oxides. From Crystal Chemistry to Physics, Wiley-VCH, Weinheim, Germany (2012).
- [2] N.B. Ivanova,, S.G. Ovchinnikov, M.M. Korshunov, I.M. Eremin, N.V. Kazak, Specific Features of Spin, Charge, and Orbital Ordering in Cobaltates. Phys.-Usp. 2009, 52, 789–810.
- [3] M. Tachibana, T. Yoshida, H. Kawaji, T. Atake, E. Takayama-Muromachi, Evolution of electronic states in RCoO₃ (R= rare earth): Heat capacity measurements, Phys. Rev. B 77 (2008) 094402.
- [4] Yu.S. Orlov, V.A. Dudnikov, M.V. Gorev, S.N. Vereshchagin, L.A. Solov'ev, S.G. Ovchinnikov, Thermal properties of rare earth cobalt oxides and of La_{1-x}Gd_xCoO₃ solid solutions, JETP lett. 103(9) (2016) 607-612.
- [5] K. Knížek, Z. Jiráček, J. Hejtmánek, M. Veverka, M. Maryško, G. Maris, T. T.M. Palstra, Structural anomalies associated with the electronic and spin transitions in LnCoO₃, Eur. Phys. J. B. 47(2) (2005) 213-220.

-
- [6] A. Ikeda, A. T. Nomura, Y.H. Matsuda, A. Matsuo, K. Kindo, K. Sato, Spin state ordering of strongly correlating LaCoO_3 induced at ultrahigh magnetic fields, *Phys. Rev. B* 93 (2016) 220401.
- [7] B. Scherrer, A.S. Harvey, S. Tanasescu, F. Teodorescu, A. Botea, K. Conder, A. N. Grundy, J. Martynczuk, L.J. Gauckler, Correlation between electrical properties and thermodynamic stability of $\text{ACoO}_{3-\delta}$ perovskites (A= La, Pr, Nd, Sm, Gd), *Phys. Rev. B* 84.8 (2011) 085113
- [8] S.K. Sahu, S. Tanasescu, B. Scherrer, C. Marinescu, A. Navrotsky, Energetics of lanthanide cobalt perovskites: $\text{LnCoO}_{3-\delta}$ (Ln = La, Nd, Sm, Gd), *J. Mater. Chem. A* 3.38 (2015) 19490-19496.
- [9] J.G. Seijas, J. Prado-Gonjal, D.A. Brande, I. Terry, E. Moran, R. Schmidt, Microwave-assisted synthesis, microstructure, and magnetic properties of rare-earth cobaltites, *Inorg. Chem.* 56.1 (2016) 627-633.
- [10] C.R. Michel, A.H. Martínez, F. Huerta-Villalpando, J.P. Morán-Lázaro, Carbon dioxide gas sensing behavior of nanostructured GdCoO_3 prepared by a solution-polymerization method, *J. Alloys Compd.* 484(1-2) (2009) 605-611.
- [11] A.S. Panfilov, G.E. Grechnev, A.A. Lyogenkaya, V.A. Pashchenko, I.P. Zhuravleva, L.O. Vasylechko, V.M. Hreb, V.A. Turchenko, D. Novoselov, Magnetic properties of RCO_3 cobaltites (R= La, Pr, Nd, Sm, Eu). Effects of hydrostatic and chemical pressure, *Physica B* 553 (2019) 80-87.
- [12] E. Olsson, X. Aparicio-Anglès, N. H. de Leeuw, Ab initio study of vacancy formation in cubic LaMnO_3 and SmCoO_3 as cathode materials in solid oxide fuel cells, *J. Chem. Phys* 145(1) (2016) 014703.
- [13] C.R. Michel, E. Delgado, G. Santillan, A.H. Martinez, A. Chávez-Chávez, An alternative gas sensor material: synthesis and electrical characterization of SmCoO_3 , *Mater. Res. Bull.* 42(1) (2007) 84-93.
- [14] H. Hashimoto, T. Kusunose, T. Sekino, Influence of ionic sizes of rare earths on thermoelectric properties of perovskite-type rare earth cobalt oxides RCO_3 (R= Pr, Nd, Tb, Dy), *J. Alloys Compd.* (2009) 484(1-2) 246-248.
- [15] V. G. Jadhao, R. M. Singru, G. Rama Rao, D. Bahadur, C. N. R. Rao, Effect of the rare earth ion on the spin state equilibria in perovskite rare earth metal cobaltates. Yttrium trioxocobaltate(III) and erbium trioxocobaltate(III), *J. Chem. Soc., Faraday Trans. 2* 71 (1975) 1885-1893.
- [16] J.W. Moon, Y. Masuda, W.S. Seo, K. Koumoto, Influence of ionic size of rare-earth site on the thermoelectric properties of RCO_3 -type perovskite cobalt oxides, *Mater. Sci. Eng. B* 85(1) (2001) 70-75.
- [17] Y. Wang, H.J. Fan, Improved Thermoelectric Properties of $\text{La}_{1-x}\text{Sr}_x\text{CoO}_3$ Nanowires, *J. Phys. Chem. C* 114(32) (2010) 13947-13953.
- [18] Z. Jiráček, J. Hejtmánek, K. Knížek, M. Veverka, Electrical resistivity and thermopower measurements of the hole- and electron-doped cobaltites LnCoO_3 , *Phys. Rev. B* 78.1 (2008) 014432.
- [19] S.R. Sehlin, H. U. Anderson, D. M. Sparlin, Semiempirical model for the electrical properties of $\text{La}_{1-x}\text{Ca}_x\text{CoO}_3$, *Phys. Rev. B* 52.16 (1995) 11681.
- [20] S. Hébert, D. Flahaut, M. Miclau, V. Caignaert, C. Martin, D. Pelloquin and A. Maignan, Search for New n-type Thermoelectric Oxides, 8th European Workshop on Thermoelectrics. 2004.
- [21] K. Iwasaki, T. Ito, T. Nagasaki, Y. Arita, M. Yoshino, T. Matsui, Thermoelectric properties of polycrystalline $\text{La}_{1-x}\text{Sr}_x\text{CoO}_3$, *J. Solid State Chem* 181.11 (2008) 3145-3150.
- [22] K. Berggold, M. Kriener, C. Zobel, A. Reichl, M. Reuther, R. Müller, A. Freimuth, T. Lorenz, Thermal conductivity, thermopower, and figure of merit of $\text{La}_{1-x}\text{Sr}_x\text{CoO}_3$, *Phys. Rev. B* 72(15) (2005) 155116.

-
- [23] L.A. Solovyov, Full-profile refinement by derivative difference minimization, *J. Appl. Crystallogr.* 37 (2004) 743-749.
- [24] A.T. Burkov, A.I. Fedotov, A.A. Kasyanov, R.I. Panteleev, T. Nakama, Methods and technique of thermopower and electrical conductivity measurements of thermoelectric materials at high temperatures, *Sci.Tech. J. Inf. Technol. Mech. Opt.* 115(2) (2015) 173–195.
- [25] K. Knížek, J. Hejtmánek, Z. Jiráček, P. Tomeš, P. Henry, G. André, Neutron diffraction and heat capacity studies of PrCoO_3 and NdCoO_3 , *Phys. Rev. B* 79(13) (2009) 134103.
- [26] O.V. Kharko, L.O. Vasylechko, S.B. Ubizskii, A. Pashuk, Yu. Prots, Structural behaviour of continuous solid solution $\text{SmCo}_{1-x}\text{FexO}_3$, *Funct. Mater.* 21 (2014) 226-232.
- [27] R. Liu, D. Xu, S. Li, Z. Lü, Y. Xue, D. Wang, W. Su, Solid-state synthesis and properties of SmCoO_3 , *Frontiers of Chemistry in China* 1(4) (2006) 398-401.
- [30] T.N. Vasil'chikova, T.G. Kuz'mova, A.A. Kamenev, A.R. Kaul', A.N. Vasil'ev, Spin states of cobalt and the thermodynamics of $\text{Sm}_{1-x}\text{Ca}_x\text{CoO}_{3-\delta}$ solid solutions, *JETP lett.* 97(1) (2013) 34-37.
- [31] V.A. Dudnikov, Yu.S. Orlov, N.V. Kazak, A.S. Fedorov, L.A. Solov'yov, S.N. Vereshchagin, A.T. Burkov, S.V. Novikov, S.Yu. Gavrilkin, S.G. Ovchinnikov, Effect of A-site cation ordering on the thermoelectric properties of the complex cobalt oxides $\text{Gd}_{1-x}\text{Sr}_x\text{CoO}_{3-\delta}$ ($x=0.8$ and 0.9), *Ceram. Int.* 44(9) (2018) 10299-10305.
- [32] A.A. Taskin, A.N. Lavrov, Y. Ando, Origin of the large thermoelectric power in oxygen-variable $\text{RBaCo}_2\text{O}_{5+x}$ ($\text{R}=\text{Gd}, \text{Nd}$), *Phys. Rev. B.* 73(12) (2006) 121101.
- [33] S.I. Vecherskii, M.A. Konopel'ko, N.N. Batalov, B.D. Antonov, O.G. Reznitskikh, T.V. Yaroslavtseva, Electrical conductivity and thermoelectric power of $\text{La}_{1-x}\text{Li}_x\text{CoO}_{3-\delta}$ ($0 \leq x \leq 0.1$) oxides, *Phys. Solid State* 58(12) (2016) 2385-2393.
- [34] J. Yu, D. Phelan, D. Louca, Spin-state transitions in PrCoO_3 investigated by neutron scattering, *Phys. Rev. B* 84(13) (2011) 132410.
- [35] S. Yamaguchi, Y. Okimoto, Y. Tokura, Bandwidth dependence of insulator-metal transitions in perovskite cobalt oxides, *Phys. Rev. B* 54(16) (1996) R11022.
- [36] S.G. Ovchinnikov, Y.S. Orlov, V.A. Dudnikov, Temperature and field dependent electronic structure and magnetic properties of LaCoO_3 and GdCoO_3 , *J Magn Magn Mater.* 324(21) (2012) 3584-3587.
- [37] Yu.S. Orlov, L.A. Solovyov, V.A. Dudnikov, A.S. Fedorov et al, Structural properties and high-temperature spin and electronic transitions in GdCoO_3 : Experiment and theory, *Phys. Rev. B* 88 (2013) 235105.
- [38] D. Stroud, The effective medium approximations: Some recent developments, *Superlattice. Microst.* 23 (1998). 567
- [39] J. Mizusaki, T. Sasamoto, W.R. Cannon, H.K. Bowen, Electronic Conductivity, Seebeck Coefficient, and Defect Structure of LaFeO_3 , *J. Am. Ceram. Soc.* 65 (1982) 363-368.
- [40] R. Kun, S. Populoh, L. Karvonen, J. Gumbert, A. Weidenkaff, M. Busse, Structural and thermoelectric characterization of Ba substituted LaCoO_3 perovskite-type materials obtained by polymerized gel combustion method, *J. of Alloys and Compounds* 579 (2013) 147–155.
- [41] T. Nozaki, K. Hayashi, T. Kajitani, Mn-substitution effect on thermal conductivity of delafossite-type oxide CuFeO_2 , *J. Electron. Mater.* 39 (2010) 1798–1802.